Supplementary Materials for

Non-contemporaneity of flow events as a control on the morphology and sedimentary character of ephemeral tributary junctions

Daniel Cadol*, Sharllyn Pimentel, David Varyu, Jonathan B. Laronne

*Corresponding author: daniel.cadol@nmt.edu
Paper DOI: 10.59236/geomorphica.v2i1.39

Table of Contents:

Supplementary Figures

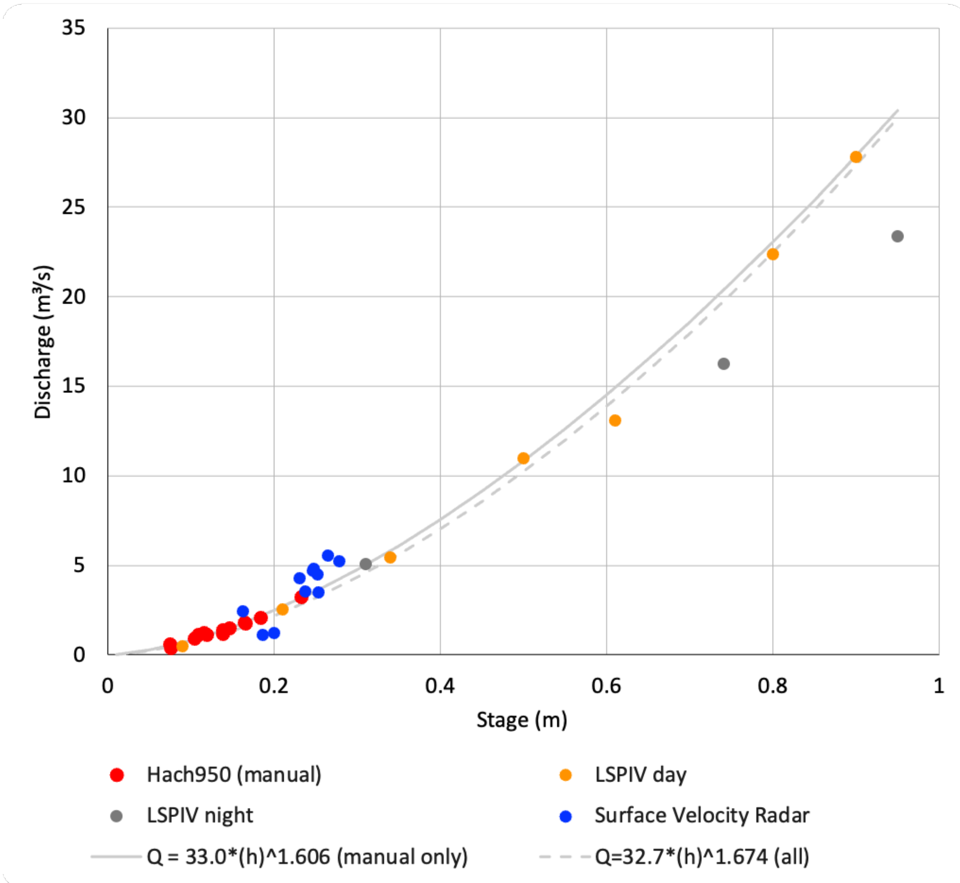

Figure S1

Stage (h) and water discharge (Q) data for the Arroyo de los Pinos. Individual discharge measurements were derived from (1) direct manual measurements of velocity across the cross section using a Hach 950 electromagnetic velocity meter, (2) surface velocity radar (SVR) measurements using a Decatur radar gun, and (3) large scale particle image velocimetry (LSPIV) measurements taken from georeferenced video footage using the Fudaa-LSPIV software package. To convert surface velocity measurements to depth-average velocity measurements, we assumed an average velocity/surface velocity ratio (alpha) of 0.85, following Le Coz et al. (2021). The resulting discharge measurements plot very close to the extrapolation from our manually measured cross section discharges. The manual measurements were undertaken at flow depths < 0.23 m, while the LSPIV measurements went up to 0.95 m depth. We found that videos recorded at night, with illumination only from oblique truck headlights, produced discharge estimates that were below the trend, which we attribute to poor video quality.

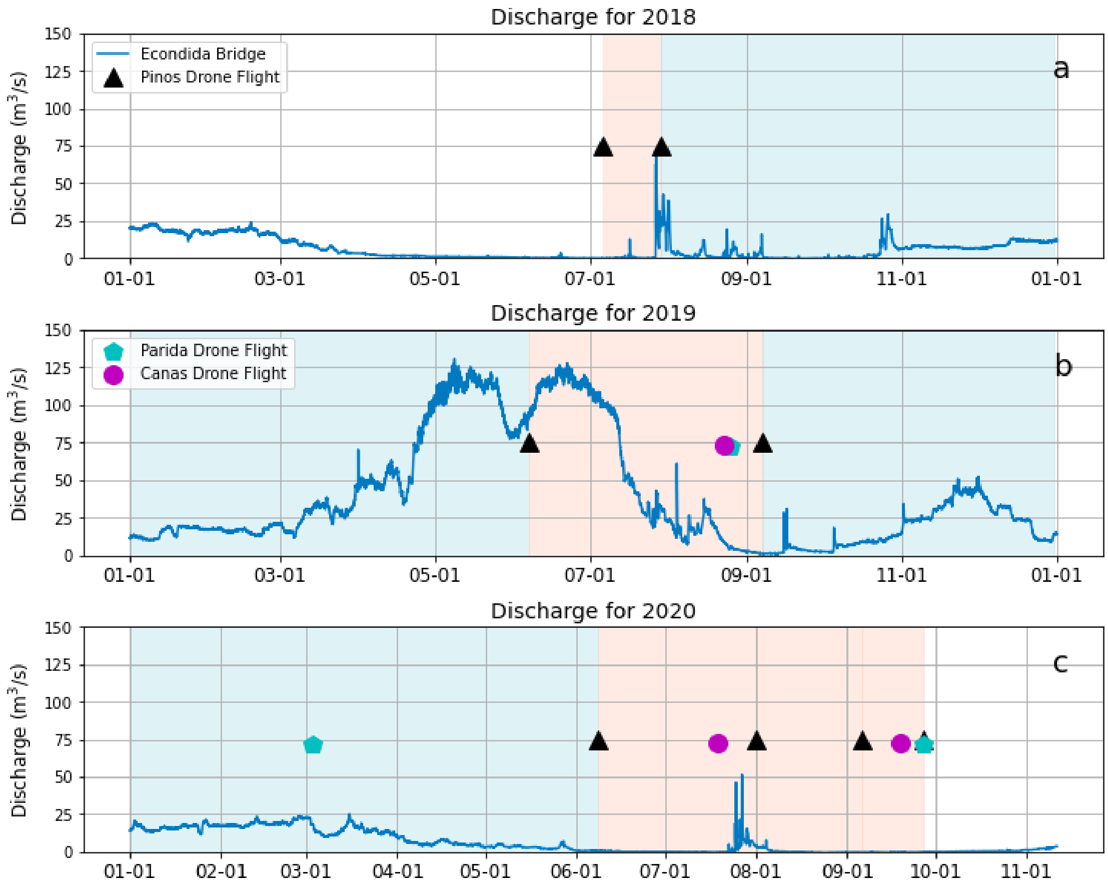

Figure S2.

Discharge hydrographs of the Rio Grande at Escondida Bridge (United States Geological Survey) 2018 to 2020. The black triangles indicated times of drone flights at the Pinos junction; blue pentagons are flights at the Parida; and circles are flights at the Cañas. The light blue and peach boxes mark the seasonal Digital Elevation Models of Difference intervals, winter and summer respectively, for the Arroyo de los Pinos surveys.

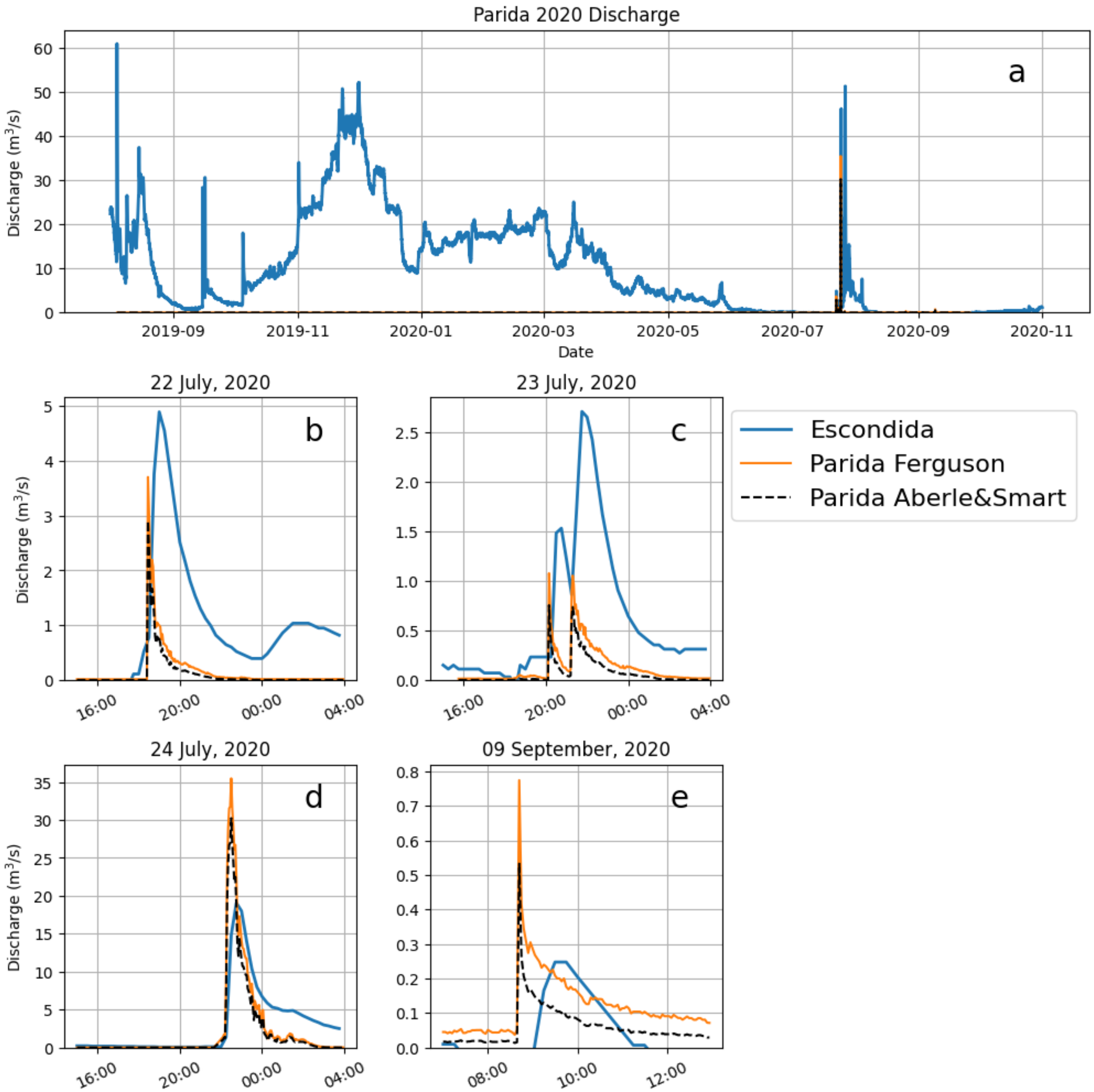

Figure S3

Water discharge of the Arroyo de la Parida and the Rio Grande at San Acacia (upstream of junction) and Escondida (downstream of junction) (a) from 2019-2020, and (b-e) during flash flood events on the Parida. The Parida discharge was estimated from stage gauging using the Manning-Strickler relationship (e.g., Ferguson, 2007) to estimate Manning's roughness parameter (n) using a roughness height equal to the 84th percentile bed material size (D_{84}), which is 12 mm at this cross section, and a bed elevation standard deviation method to estimate the roughness parameter as proposed by Aberle and Smart (2003).

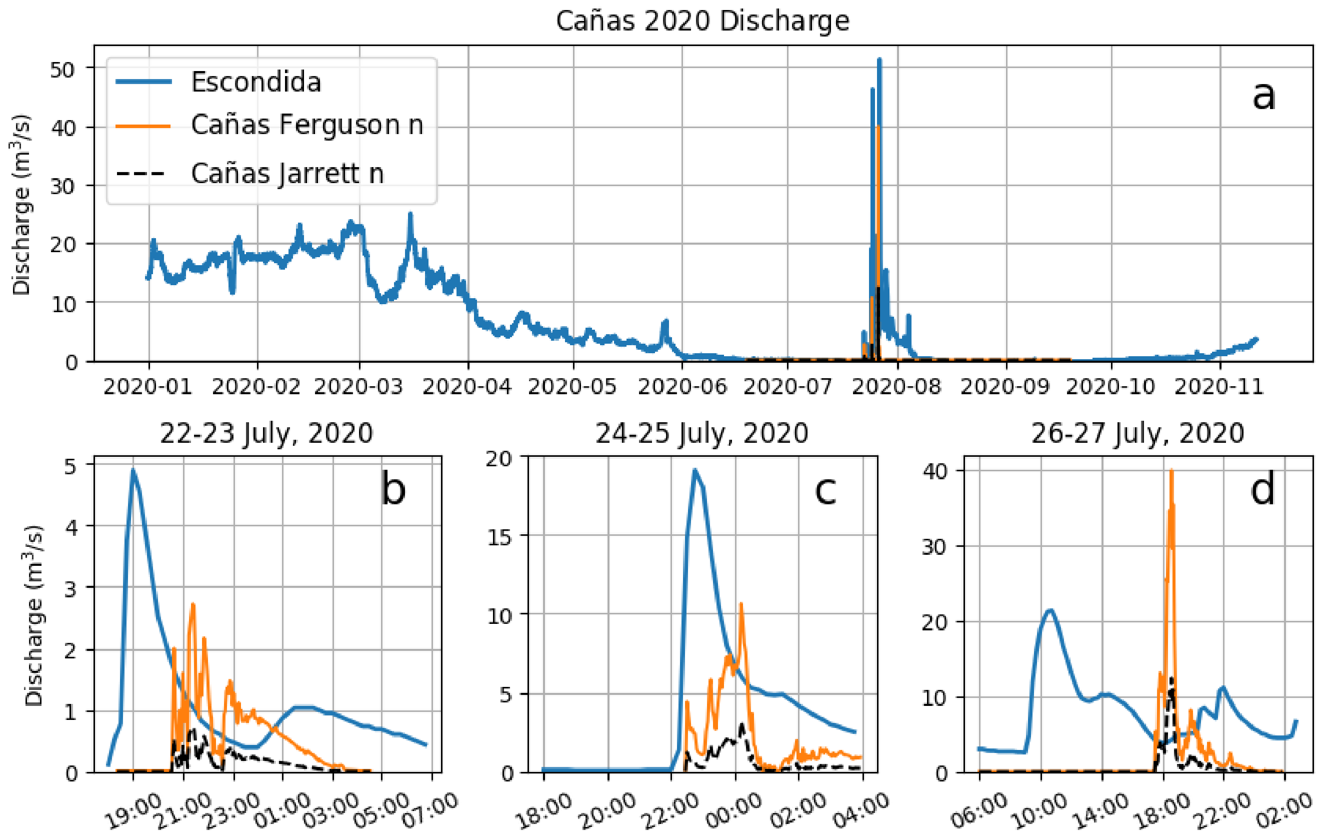

Figure S4

Water discharge of the Arroyo de las Cañas, using two methods of finding Manning's roughness parameter (*n*), and the Rio Grande at Escondida 13 km upstream of junction (a) during 2020, and (b-d) during flash flood events on the Cañas. The Cañas water discharge was estimated from stage gauging using the Manning equation, with *n* estimated using the Manning-Strickler relation (e.g., Ferguson, 2007) with roughness height equal to the 84th percentile bed material size (D_{84}), which is 22 mm at this cross section, and the steep channel method of Jarrett (1984).

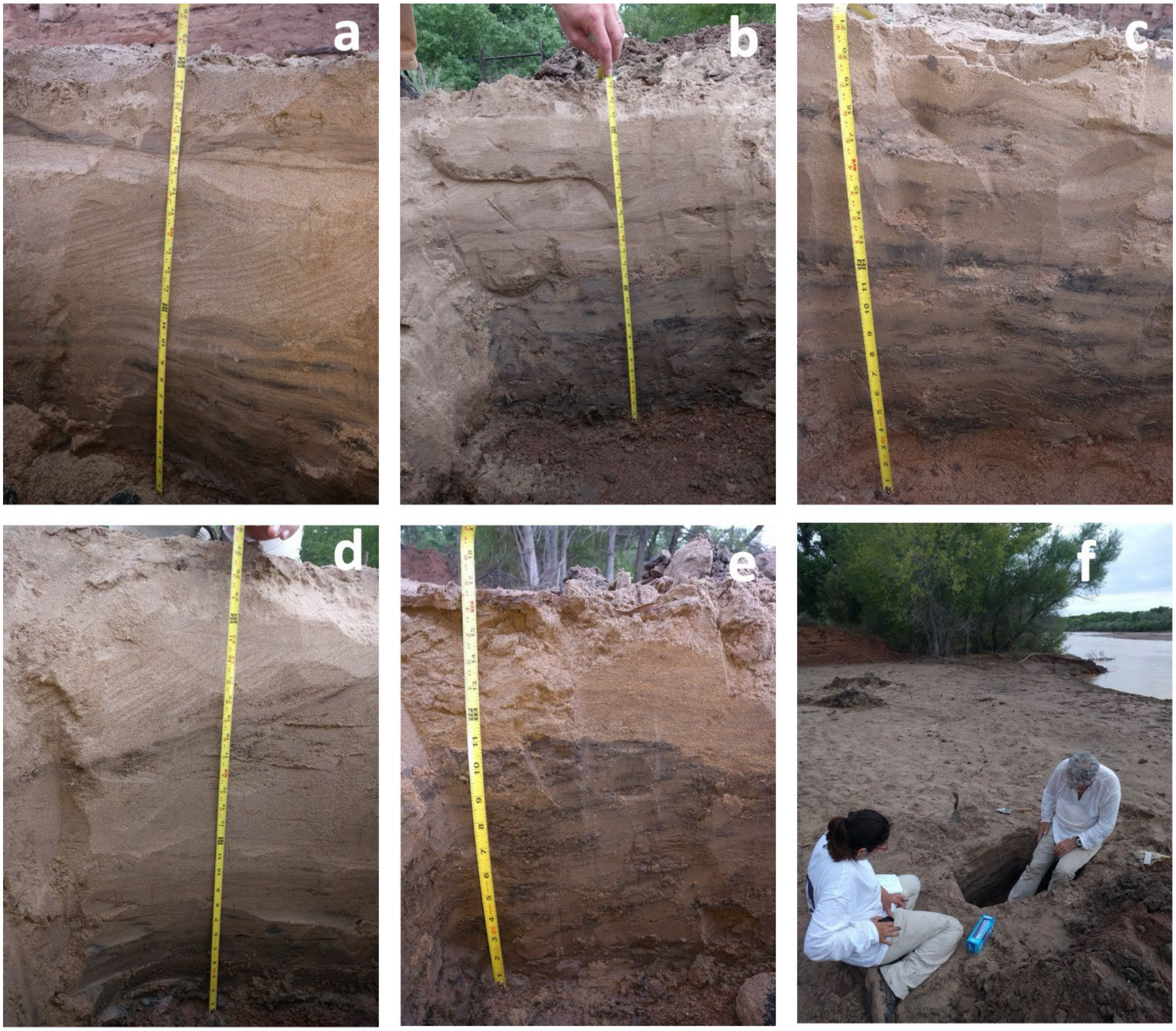

Figure S5

Photographs of sediment sampling pits on the Arroyo de los Pinos mouth bar, 6 August 2019. All views of pit wall are looking southward. Note the unsampled gravel-rich deposit at the bottom of each pit, marking the lower limit of mouth bar deposition and the top of the tributary flood deposits. The tape measure in each photo is marked in feet and inches. a) South Sandbar location (for map of locations, see Figure 4); note eastward dipping bedding in middle, capped by finer material. b) Center Sandbar location; thinner east-dipping bedded section than in the south pit. c) North Sandbar location; minimal dip angles and interbedded silts and sands in lower section. d) East Sandbar location; east-dipping sand beds overlie more massive sand deposit. e) West Sandbar location; closest to river, slight dip to the west in the sand cap over finer silt-dominated deposit. f) South-southwest view of the North Sandbar pit; Center pit in background; West pit is not yet excavated but would have been in the view; Rio Grande in background flows south away from camera location.

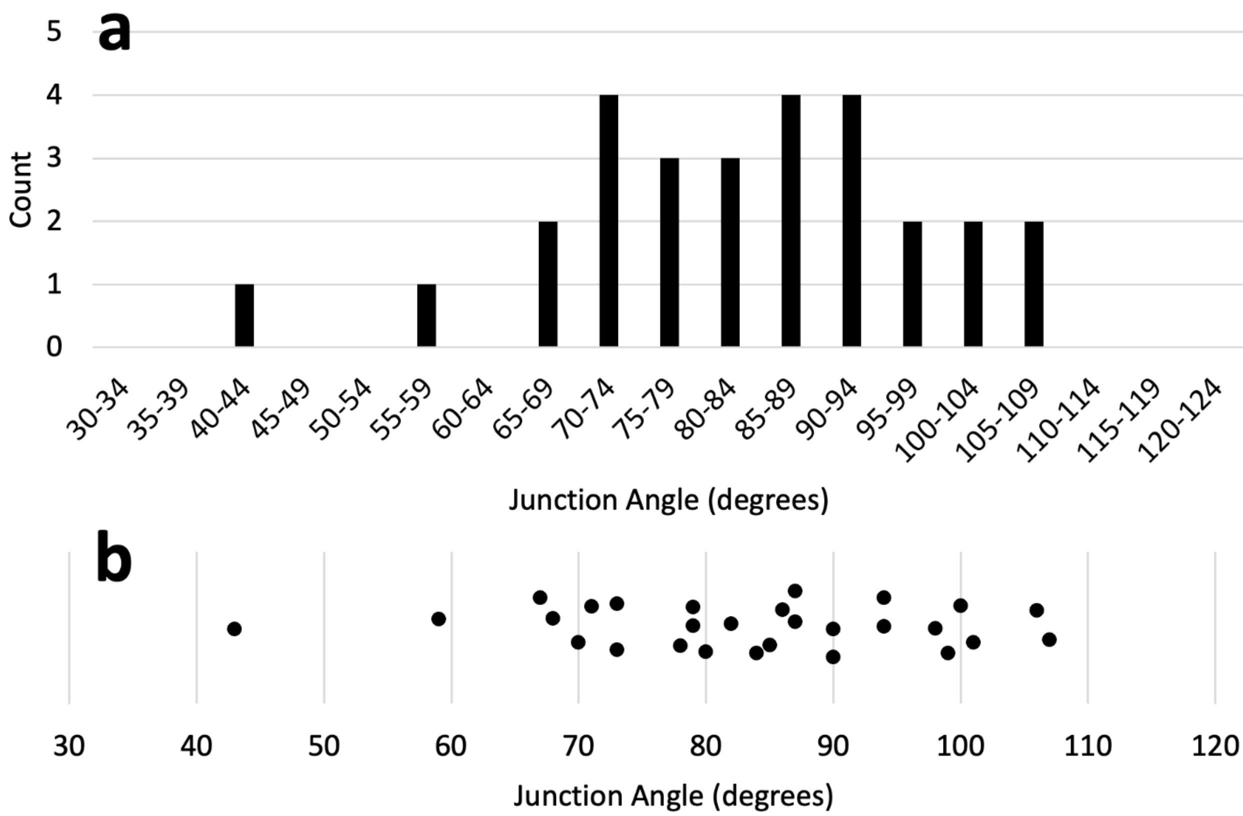

Figure S6

Junction angles of tributaries to the Rio Grande in the reach below Cochiti Dam (Santa Fe River) downstream to below Elephant Butte Dam (Palomas Creek). Data were collected using aerial photographs available on Google Earth. a) Histogram of measured junction angles. b) Population distribution of the 28 identified and measured junctions.

Supplementary Tables

Table S1

Manual discharge measurements at Arroyo de los Pinos, with calculated *n*-values and equivalent D_{84} grain size of the roughness.

Date	Stage (m)	Discharge (m^3/s)	Resulting n^*	Equivalent grain diameter (mm)
07 July 2018	0.23	3.22	0.028	75
07 July 2018	0.18	2.09	0.029	99
07 July 2018	0.15	1.51	0.028	74
07 July 2018	0.14	1.21	0.031	162
07 July 2018	0.08	0.39	0.037	412
09 Aug 2018	0.14	1.38	0.028	75
09 Aug 2018	0.10	0.92	0.026	56
09 Aug 2018	0.07	0.58	0.024	29
23 July 2020	0.17	1.74	0.029	110
23 July 2020	0.12	1.14	0.025	41
23 July 2020	0.12	1.23	0.023	26
23 July 2020	0.17	1.80	0.028	86
23 July 2020	0.11	1.15	0.022	21

* The average *n* of these measurements is 0.028, giving an equivalent grain size of 74 mm. Based on sieving of large quantities of bed material, this is equivalent to the D_{96} of the bar material and the D_{98} of the thalweg, and notably coarser than the measured D_{84} of 16 mm in the thalweg and 48 mm in the bars (spatial average of 22 mm).

Table S2

Equivalent *n* values for different flow estimation methods.

Arroyo	Event	Manning-Strickler *n* (Ferguson)	Aberle & Smart *n*	Jarrett *n*	Rating Curve *n*	Q_{peak} (m^3/s) Manning-Strickler	Depth at thalweg (m)
Pinos	16 July 2018	0.022	0.028	NA	0.026	12.0	0.48
Pinos	26 July 2018	0.022	0.023	NA	0.031	96.7	1.59
Pinos	09 Aug 2018	0.022	0.039	NA	0.026	2.4	0.18
Pinos	24 Aug 2018	0.022	0.033	NA	0.027	5.1	0.28
Pinos	01 Sept 2018	0.022	0.049	NA	0.026	1.3	0.12
Pinos	23 July 2020	0.022	0.039	NA	0.026	2.4	0.18
Pinos	24 July 2020	0.022	0.032	NA	0.027	5.7	0.30
Pinos	01 Sept 2020	0.022	0.045	NA	0.026	1.5	0.13
Parida	22 July 2020	0.020	0.025	0.053	NA	3.7	0.40
Parida	23 July 2020	0.020	0.029	0.057	NA	1.1	0.27
Parida	24 July 2020	0.020	0.023	0.043	NA	35.5	0.96
Parida	09 Sept 2020	0.020	0.029	0.059	NA	0.8	0.02
Cañas	22 July 2020	0.022	NA	0.087	NA	2.7	0.32
Cañas	24 July 2020	0.022	NA	0.077	NA	10.6	0.51
Cañas	26 July 2020	0.022	NA	0.074	NA	39.8	0.85